TRANSPORT AND RESEALING DYNAMICS OF TWO PULSE ELECTROPORATION MEDIATED MOLECULAR DELIVERY

By

YASIR DEMIRYUREK

A thesis submitted to the

Graduate School-New Brunswick

Rutgers, The State University of New Jersey

In partial fulfillment of the requirements

For the degree of

Master of Science

Graduate Program in Mechanical and Aerospace Engineering

Written under the direction of

Prof. Jerry W. Shan

And approved by

_____

_____

_____

New Brunswick, New Jersey

October, 2014

ABSTRACT OF THE THESIS

Transport and resealing dynamics of two pulse electroporation mediated molecular delivery

by Yasir Demiryurek

Thesis Director: Prof. Jerry W. Shan

Electroporation-mediated molecular delivery is of interest for many drug-delivery and gene-therapy applications. Recent studies have shown that a two-pulse protocol consisting of a short-duration high-voltage first pulse followed by a longer, low-voltage second pulse can increase the efficiency of molecular delivery and preserve more cells alive with suitably chosen pulsing parameters. In this work we investigate the effects of the first and second pulses' field strength and the inter-pulse delay time on the delivery of two different-sized Fluorescein-Dextran conjugates (10 kDa and 70 kDa). A series of two-pulse electroporation experiments were performed on 3T3 mouse fibroblast cells, with an alternating-current first pulse to permeabilize the cell, followed by a direct-current second pulse to electrophoretically deliver the target molecule into the cell. Our results showed that the delivery amounts of Fluorescein-Dextran varies strongly with the first pulse's field strength and target molecule size. By varying the delay times between two pulses, it is shown that the delivered intracellular concentration of Fluorescein-Dextran decreased linearly with the logarithm of delay time. The data also indicate that

membrane resealing after electropermeabilization occurs very rapidly, but that a non-negligible fraction of the pores can be reopened by the second pulse for times on the order of 100s. The role of the second pulses is seen to be more than just electrophoresis, with a minimum threshold field strength required to reopen nano-sized pores or defects remaining from the first pulse. These results suggest that membrane electroporation, sealing, and reporation is a complex process that has both short-term and long-term components, which may in part explain the wide variation in membrane-resealing times reported in the literature.

Acknowledgements

I would like to begin thanking my advisor, Dr. Jerry W. Shan. I am grateful that he continually and convincingly conveyed a spirit of adventure in regard to my research. I would also like to express my deepest appreciation to my co-advisors and committee members, Dr. Hao Lin, Dr. David Shreiber, and Dr. Jeffrey Zahn for supporting and motivating my thesis work. I would not be able to navigate in this research field without their guiding light and their enormous point of view in their field. I also thank my undergraduate advisors Dr. Mehmet Ali Guler and Dr. Unver Kaynak for guiding me to construct a firm ground of engineering perspective.

I owe a debt of gratitude to all many previous and current colleagues from both Mechanical and Biomedical Engineering departments, especially Cevat Akin, Mohamed Sadik, Mingde Zheng, Miao Yu, Gabriel Giraldo, Wuhan Yuan, Rick Castellano, Sagar Singh, Masoud Nickaeen, Kaiyan Yu and Semih Cetindag for being utmost helpful and supportive during my research journey. I would also like to thank several of my fellow graduate students who have been a source of inspiration and encouragement over the years. First, I would like to thank Gokhan Simsek, Nazim Babacan, Onurhan Ozcelik, and Mustafa Gun who have been a strong companion through my undergraduate studies, and Arturo Villegas Vaquero, Joseph Cullen O'Connor, Moiz Ezzy, Sunny Wong, Matthew Frenkel, William Mozet and many others for consulting through my graduate studies. I would like to express my sincere gratitude to Yusuf Turhan for being the most supportive companion during my research experience. Lastly and undoubtedly, I specially thank to my roommates Cevat Akin and Arturo Villegas Vaquero not only for

being the excellent friends, but also building the family warmth at home and becoming more than a friend to me.

Finally, but the most important, I thank my family for being so supportive, encoring and always making me aware of their priceless love. I owe my deepest gratitude to my parents, Alaaddin and Nahide Demiryurek and my sister Arife Erturun, and my girlfriend Giselle Figueroa Gonzalez.

Dedication

To my parents Alaaddin and Nahide Demiryurek

Table of Contents

List of Tables

List of Figures

Chapter 1

Introduction

Electroporation-mediated molecular delivery has shown a great enhancement in various applications for gene transport, or protein or drug delivery among many other biochemical methods [1–9]. In principle, this phenomenon can be considered in two main aspects; (I) electro-permeabilization of the membrane and (II) electro-transportation of target molecules. The presence of suitably chosen external electric field permeabilizes the cell membrane and introduces foreign molecules into the cell cytoplasm [10–14]. However the major disadvantage of this procedure is the death of a significant portion of the cell population due to high voltage application. To overcome this limitation, among various techniques, a two-pulse protocol is used to increase the efficiency of molecular delivery and preserve more cells alive with suitably chosen pulsing parameters [15–29]. However, the lack of fully understanding the effect of pulsing parameters still attracts interest of researchers seeking to understand the fundamental mechanisms and optimize delivery and viability. At this point, this thesis provides a distinct pulsing design in order to separate permeabilization and delivery clearly and allows us to analyze each mechanisms separately. The main focus of this work is to study the effect of the permeabilization pulse field strength and delay time between two pulses on molecular delivery of two different-sized Fluorescein-Dextran conjugates (10 kDa and 70 kDa).

1.1. Mechanisms of Electroporation-Mediated Molecular Delivery

In earlier works, it has been reported that in the presence of external electric field some type of electrical breakdown occurs in the cell plasma membrane [30] and consequently

the conductance of the membrane increases dramatically [31]. These findings showed that, when an external electric field is applied to the cell membrane, after reaching a critical threshold transmembrane potential, the cell membrane no longer behaves like an insulator, becomes more conductive and allows the extra-cellular foreign molecules to pass through into cytoplasm. E. Neumann et al. performed the first gene transfer into mouse lyoma cells by applying suitable electric pulses and presented a simple, easy applicable and efficient way to transport genes into the cells compared to other biochemical techniques [1]. After that, electroporation-mediated molecular delivery has become a hot research area for researchers seeking to understand the fundamental mechanisms and optimize delivery and viability.

Electroporation-mediated molecular delivery can be considered in two main aspects; (I) electro-permeabilization of the membrane and (II) electro-transportation of target molecules. It is shown that, for both mechanisms the electrical parameters clearly play applied important role [32,33]. Therefore this study and as many other studies focused on the electrical pulsing parameters in order to better understand the mechanism and improve the efficiency [15,17,20,28,34–54]. Although other physiological [55–58] and cellular [59–62] effects help to improve the electroporation (EP) procedure, those effects are not scope of this study.

1.1.1. Electropermeabilization of the cell membrane

An application of suitably chosen electric pulse to the cell membrane transiently increases the permeability of the membrane. It has been shown that the electrical breakdown of the membrane occurs after reaching a critical transmembrane potential [34–37]. Also depending on the pulsing parameter, this permeable stage occurs either

temporary (reversible) or permanently (irreversible). These reversible and irreversible electropermeabilization have different application areas, for example in the applications of debacterialization or ablation of solid tumors irreversible electropermeabilization is used [63–66], where in the application of drug delivery or gene therapy reversible electropermeabilization is used [1–9]. In order to understand the permeabilization mechanism, it is important to know bilayer lipid structure of the membrane. Due to nature of the lipid molecules, the cell membranes functions as a combined resistor and capacitor [67]. Therefore in the application of an external electric field, the membrane is charged as a capacitor due to accumulation of ions from the surrounding solution [68]. When the applied pulse surpass the capacitance of the membrane, electropermeabilization takes place [34–37]. Maintaining the field strength over critical threshold value expands the permeabilization of the membrane. This process is explained as "induction step" and then "expansion step", where in the induction (trigger) step, the applied pulse induces a potential difference across the membrane until a critical threshold value, and creates small defects on the membrane (nucleation sites), and then in the expansion step, it extends those defects until a potential equilibrium is reached [69]. Experimentally, these procedure is shown by Hibino et al. by using voltage-sensitive dyes [36,37]. In fact, this dynamic process of pore evolution and statistical distribution is well captured by Smoluchowski equation (SE) as a function of transmembrane potential. In many EP modeling study, this equation is solved to stimulate the pore evolution [70–72]. As a result, those extensive researches has established a mature understanding for electropermeabilization stage.

Many previous studies have shown that, adjusting pulsing parameters, including field strength [28,40–46], pulse duration [38,41,44,47], number of pulses [15,48,49], and pulse shape [50–54] have changed the degree of permeabilization. Understanding the effect of these parameters provided an optimization path, particularly for reversible EP protocol where a high viability ratios were required. As is known, the major drawback of the EP is the death of a significant portion of the cell population due to high voltage application. To overcome this limitation, among various techniques, a combination of a short-duration high-field strength pulse with a longer-duration lower-field strength pulse can increase the EP efficiency and preserve more cells alive [15–29]. We will discuss this method in more detail in a separate section.

1.1.2. Electro-transportation of the target molecules

Electro-transportation is another important aspect of EP phenomenon. Many experimental works provided a variety of knowledge about molecular uptake. However due to its complexity, a comprehensive understanding of transport mechanism is still under investigation. It has been shown that molecular delivery strongly depends on the type or size of the target molecule [19,73,74]. Besides, this mechanism not only depends on the electrophoresis, but also involves different mechanisms depending on the target molecule. For instance, the transport of small molecules (MW < 4 kDa) involves both dynamic diffusion and electrophoresis [75]. This process can be modeled by the Nernst-Planck (NP) equation [39]. On the other hand, the transport of large molecules (MW > 4 kDa) such as DNA involves endocytosis, DNA-membrane interaction, electrophoresis, and maybe more unknown mechanisms [76,77]. Thus transport of large molecules requires more work to have a full understanding. Based on the current knowledge, it has

been recognized that the main molecular uptake of moderate and large molecules occurs through electrophoresis [15,20,28,38,39]. Therefore, prolonging the applied pulse duration, increases the delivery amount significantly [78,79]. In fact, our previous colleague found a linear relation between the delivery amount and the duration of the pulse [19]. However, longer pulse durations decreases the viability ratio, and causes unfixable damages on the cell membrane. We believe that many of the cell death happens due to over-poration of the membrane, which subsequently causes rupturing of the membrane or losing the integrity of the cell. To overcome this limitation, permeabilization and delivery should be separated and different pulsing parameters should be applied. For example, a high degree of permeabilization can be achieved by a strong pulse in very short time, while delivery can be persisted by a weaker and longer-duration pulse. Indeed, this procedure (two-pulse electroporation) has been used by many researchers. However, the effect of pulsing parameters have not understood completely due to ambiguity of presented works.

1.2. Two-pulse Electroporation protocol

As stated before, the EP phenomenon consists of two main aspects (permeabilization and molecular-transport), and they are determined by the electrical parameters of applied field in spite of the fact that different physical mechanisms are involved for both. Indeed, permeabilization and delivery require different kinds of pulse parameters, for example, in order to permeabilize the membrane the critical transmembrane potential threshold must be exceeded, where in some cases (particularly for larger molecules), this threshold might be higher. On the other hand for delivery, longer pulse duration is required instead of a stronger pulse [78,79]. To resolve this contradiction, EP pulse is split into two different

pulses which are a short-duration high-field strength pulse for permeabilization and a longer-duration lower-field strength pulse for delivery (denoted by 'HV' and 'LV', respectively) [15–29]. In this two-pulse procedure, permeabilization and delivery are considered to be separate task, with the first HV pulse inducing a high level of permeabilization, followed by a second LV pulse that increases the delivery amount due to electrophoresis. Many researchers have studied the pulsing parameters such as first pulse's (FP) field strength [18,20,28], the second pulse's (SP) field strength and duration [15,16,18,19,21], and delay between pulses [15–18,29,79], in order to better understand the fundamentals of two-pulse EP and optimize transfection efficiency.

Those studies showed that the efficiency of the multi-pulse EP delivery is strongly depended on the pulsing parameters. For instance, tuning the FP field strength and duration varied the EP efficiency drastically. As expectedly, increasing the field strength and duration of the FP increased the molecular delivery efficiency until a critical point, where too high field strength or too long duration of the FP decreased the EP efficiency due to low viability ratio [18,20,28]. In order to maintain high viability, Cukjati et al. developed an algorithm that monitors the current-voltage responses in real-time and adjusts the field strength of the FP, however this algorithm does not provide a desired level of permeabilization for delivering different sized-molecules since the size of electro-pore cannot be measured [28]. In addition the FP, the effect of the SP field strength and duration have also been studied [15,16,18,19,21]. In particular, a recent study has examined the scaling behavior of two-pulse delivery and viability by varying the field strength and duration of the SP (E_2= 0.1 - 1 kV/cm, t_2= 10 - 100 ms) [19]. This study found a linear relation between the delivery and the duration of the SP and an

inverse linear correlation between viability and electrical energy, allowed simultaneous optimization of delivery and viability. However, that work focused on the SP parameters, and did not study other pulsing parameters such as the delay between pulses. Lastly, another parameter, the delay time between two pulses has been also studied in order to understand DNA-membrane interaction mechanisms [16–18,29] or resealing mechanism [15,16,79]. In most of those works, delay time effect on molecular delivery has not been studied quantitatively, few works have performed a systematic study that delay time ranges from milliseconds to hundreds of seconds. However, the effect of the delay time has not been understood fully due to controversial results. For example, an earlier work by Sukharev et al. showed that the transfection efficiency was decreased when the delay between pulses was increased [15], while Satkauskas et al. showed that an optimum transfection have been reached at between 0.3 to 100s delay time [16]. Additionally, most of those works have studied on electro-transfection of genes which involves gene-membrane complex formation, thus the amount of the delivery was not solely depended on electrophoresis and hard to quantify accurately. Furthermore, most of those studies on multi-pulse EP have focused on direct-current (DC) fields only, thus permeabilization and delivery have not studied separately due to electrophoretic drift of the DC pulses. As shown in many studies [15,17,19,20,22,27], the HV pulse alone can transport a considerable amount of the target molecule, confounding permeabilization and delivery. To overcome this limitation, we use an alternating current (AC) electric field for the FP coupled with a DC SP to achieve a clear separation of permeabilization and delivery.

1.3. Statement of Objectives

This thesis investigates the effect of the FP field strength and delay time between two pulses on EP-mediated molecular delivery. Additionally, the effect of molecular size in the transport mechanism is also studied by using different-sized Fluorescein-Dextran (FD) conjugates (a non-binding chain polymer), with molecular weights of around 10 kDa and 70 kDa. Due to its non-binding nature and similar size range, dextrans can be more correlated with RNA or peptides in terms of electrophoretic transport and total permeabilized area on the membrane [38]. It is also shown that the transport of mid-sized molecules is directly correlated with the state of permeabilization [19] which avoids the complexity induced by the dynamic diffusive process associated with smaller molecules. The specific objectives of this work are to:

1. Separate permeabilization and delivery clearly by employing a high-frequency AC FP with a DC SP.
2. Demonstrate the effect of the degree of permeabilization on molecular transport by varying the field strength of the FP.
3. Compare the electro-pore sizes obtained by different field strength by delivering different-sized target molecules.
4. Study the effect of the delay times between pulses systematically by ranging delay times from milliseconds to hundred seconds.

Distinct work, firstly, we employ an AC field FP to achieve a clear separation of permeabilization and delivery, thus that allows us to analyze each mechanisms separately. Secondly, taking advantage of non-binding mid-sized FD we can directly correlate the delivery with the degree of permeabilization and on top of that different-sized molecules

allows us to investigate the size of electro-pores. Finally, our pulse design provides us to probe the resealing dynamics of the cell membrane systemically.

In the following chapters, experimental setup and procedure (Chapter 2) is given, followed by our experimental results for two-pulse electroporation mediated molecular transport (Chapter 3) and then a vast discussion of our results (Chapter 4). In the final part, a conclusive summary and suggestions for the future work is included in this thesis (Chapter 5).

Chapter 2

Materials and Methods

In this thesis, a series of two-pulse electroporation experiments were performed on 3T3 mouse fibroblast cells, with an alternating-current first pulse to permeabilize the cell, followed by a direct-current second pulse to electrophoretically deliver the target molecule into the cell. This chapter explains the experimental setup and procedures.

2.1. Cell Culture

NIH 3T3 mouse fibroblast cells were used throughout the experiments and cultured in Dulbecco's Modified Eagle Medium (DMEM) supplemented with 10% Fetal Bovine Serum (FBS), 1% Penicillin-Streptomycin, and 1% L-Glutamine (Sigma-Aldrich, St. Louis, MO) and incubated at 37°C and 5% CO_2. The reason for choosing this 3T3 cell line is because they are easy to culture and well suited for transfection studies [80]. Approximately 3×10^6 cells were trypsinized at 70-80% confluency with 0.5% trypsin/EDTA (Sigma-Aldrich) followed by centrifugation for 2 minutes at 2000 rpm (Allegra X-21, Beckman Coulter, Brea, CA) in culture media, and then twice in electroporation buffer containing 0.4 mM $MgCl_2$, 250 mM sucrose, and 10 mM HEPES (Sigma-Aldrich) (pH 7.4). It is noted that, the optimum confluency of the cell population is usually reached after three days of the cell passage. The osmolarity and electrical conductivity are measured with osmometer (3D3 Osmometer, Advanced Instruments, Norwood, MA) and conductivity meter (CON 6, Oakton Instruments, Vernon Hills, IL), and adjusted to 310 mOsm/kg and 100 μS/cm, respectively. The osmolarity is kept almost the same with the intra-cellular osmolarity in order to avoid swelling after EP. It is

also shown that lower extra-cellular electrical conductivities increased the delivery. This physiological effect which called FASS is well explained in the Sadik et al. [58].

2.2. Electroporation Setup

The cell suspension was subjected to electric pulses in an EP cuvette with a 1-mm electrodes gap (VWR, Radnor, PA) at room temperature (20°C) under a sterile hood. Electric pulses were generated by a function generator (Tektronix AFG3022C, Melrose, MA) and amplified by a high-frequency, high-voltage amplifier (Trek Model PZD 350, Lockport, New York, NY) (Figure 2. 1a). Applied pulses were measured by oscilloscope (PicoScope 5203, Cambridgeshire, UK). It is experienced that, attaching the oscilloscope directly to cuvette-electroporator with an 10X attenuated probe provides more accurate measurements instead of monitoring from the amplifier outlet. Figure 2. 1a shows connection order of the electronic devices schematically. In Figure 2. 1b, an example of generated AC + Delay time + DC pulse shape is shown.

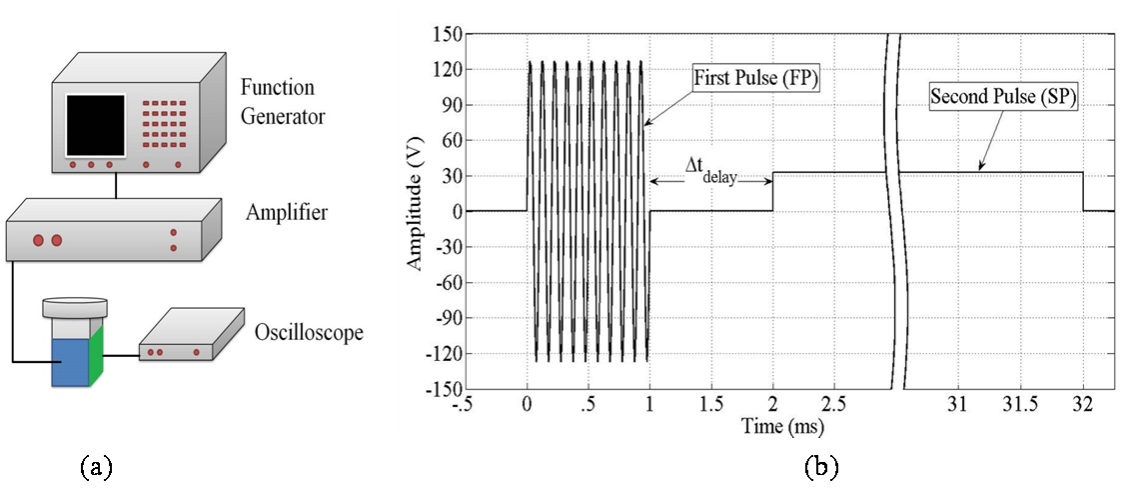

Figure 2. 1. Schematic of (a) the experimental setup and (b) AC first (FP) and DC second (SP) pulses applied to the cells with a specified delay.

2.3. Electroporation Procedure

The cells were suspended in the EP buffer including 100 μM of Fluorescein-Dextran (FD) (Life Technologies, Grand Island, NY) and kept in the ice for 5 to 15 minutes before applying pulses. Two different FD conjugates with a molecular weight of around 10 kDa and 70 kDa were utilized to measure delivery. In most of the experiments, two consecutive different pulse were applied to the cells; an AC first pulse (FP) for cell permeabilization and a DC second pulse (SP) with some delay for FD delivery (Figure 2. 1b). The pulse parameters (shape, strength and duration) are given in Table 2.1. For each experiment, control cases were also studied in which cells were treated to every step of experiment, but without exposure to the electroporation pulses. The delay times (Δt_{delay}) between two pulses were arranged by the function generator's Trigger Delay option between two channels and precise delays ranging from no delay to milliseconds to seconds were obtained. Delay times longer than 80 seconds (such as 100 s and 300 s delays) were timed with a stopwatch and applied manually. Immediately after pulsation, culture media was added to the cell suspension and incubated for 30 minutes to allow for resealing. Then, the cell suspension was transferred to phosphate buffer saline without Mg^{2+} and Ca^{2+} (PBS) (Sigma-Aldrich) containing 2 μM of 7-Aminoactinomycin D (7-AAD) (MW = 1270.43 Da) (Life Technologies) solution in order to determine viability (53) and waited for 15-20 minutes. 7-AAD, which is used for staining nucleic acids, is a cell-membrane-impermeant dye. However, the cells that were not able to recover and reseal after pulsation do uptake 7-AAD which fluoresces upon binding to nucleic acids. Thus, cells which allowed 7-AAD entry after 30 minutes were considered to be dead cells. The cell suspension was washed twice with PBS in order to remove free FD and

unbounded 7-AAD before fluorescence imaging. All experiments were repeated at least 3 times for consistency, and for each experimental condition at least 100 cells were analyzed.

Table 2.1. Applied pulse parameters for the first and second pulse

	First Pulse (FP)	Second Pulse (SP)
Shape	AC Sinusoidal (f = 1- 500 kHz)	DC
E. Field Strength	E_1= 0.60 - 0.90 kV/cm	E_2= 0.33 kV/cm
Duration	t_1= 1 ms	t_2= 30 ms
Delay between FP and SP	0 - 300 s	

2.4. Fluorescence Imaging Microscopy

Both FD and 7-AAD fluorescence signals were acquired using fluorescence-imaging microscopy. The cell images were taken by a high-sensitivity camera (pco.edge sCMOS, PCO AG, Kelheim, Germany) attached to an inverted microscope (Olympus IX71, Center Valley, PA) with a 20x objective. Approximately 20 μL of cell solution was dropped between two cover slip was placed on top of motorized stage. The cell solution was sandwiched between two cover slip solution in order to obtain standard thickness (approximate cell diameter: 15 μm) and avoid cell motion due to flow. A high intensity discharged mercury vapor lamp is used as an illumination source for imaging. That UV light is filtered by a triple-band excitation filter (DAPI - FITC - TRITC), and exposed to the cell solution. Then using the appropriate emission filter, the signal of the fluorophore is captured by camera. The cell images were taken with two different fluorescent channel (for FD ex: 494nm, em: 521nm, for 7-AAD ex: 488nm, em: 647nm). Additionally, one bright field image was also taken to detect the cell diameter and center coordinates for image processing. The cell solution was controlled by a motorized stage and programmed

to take a series a patterned images. The fluorescence light's shutter was controlled manually and elaborated to avoid photo-bleaching. Figure 2.2 shows the working principles of the fluorescence imaging technique schematically.

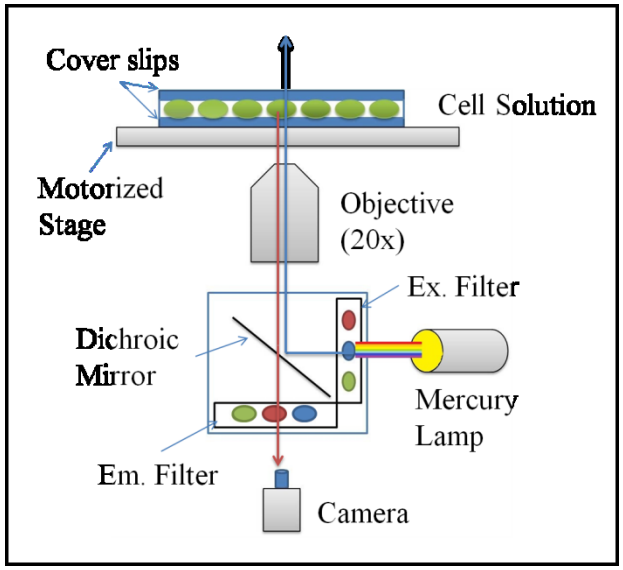

Figure 2.2. A schematic of working principle of fluorescence imaging. A high-intensity UV light which is provided by a mercury lamp, is filtered by triple band pass (DAPI - FITC - TRITC) filter and images are acquired by a high-sensitivity camera.

2.5. Image Processing and Data Analyzing

Figure 2.3a shows an exemplary set of images which were taken in the bright-field, FD-fluorescence, and 7-AAD-fluorescence channels, from the top to bottom rows respectively. All images and data were analyzed with MATLAB (The MathWorks, Natick, MA). The code is given in Appendix A. The bright-field images (Figure 2.3a) were used to compute a disk-shaped profile for each cell and detect the cell's center coordinates and diameter. Fluorescence intensity per volume for each cell is calculated by integrating the signal within the disk shape area and normalized by the cell volume. Then the background noise that calculated from a control (no-pulse) case was subtracted from

the other cases. This was done for both the FD channel and 7-AAD channel to determine the fluorescence intensities for each individual cell.

The scatter plot shown in Figure 2.3b has FD intensity per volume (corresponding to the degree of delivery) as its abscissa, and 7-AAD intensity per volume (related to the viability of the cell) as its ordinate. As previously mentioned, 7-AAD was used to detect dead cells, and the cells that were above the viability line were presumed to be non-viable. The level of the viability line was determined by 7-AAD intensities two standard deviations above the mean fluorescence intensity. For analysis of the delivery of FD, only alive cells were considered. Throughout the experiments, viability was above 80% in many cases and always exceeded 60%.

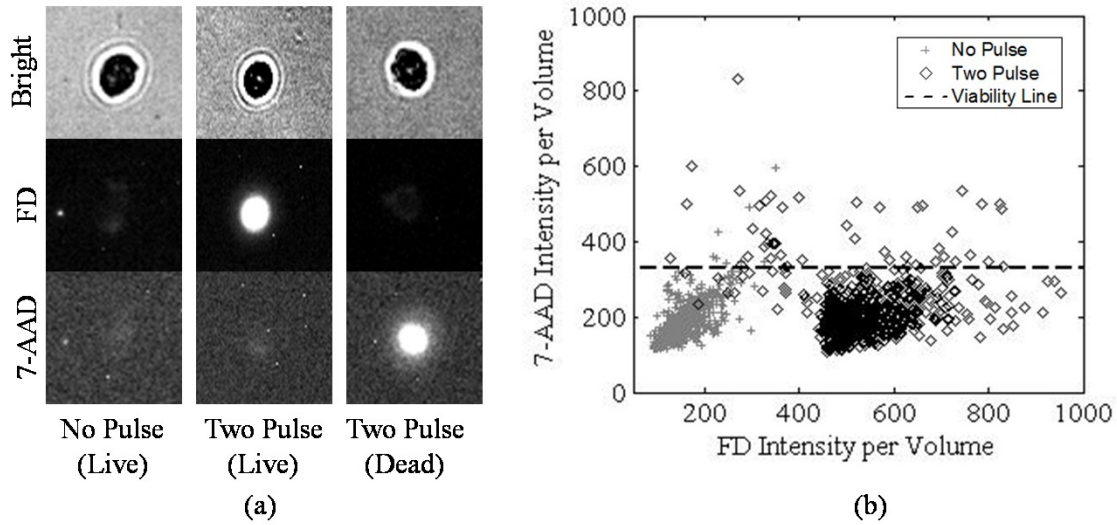

Figure 2.3. Examples of (a) cell images taken for image processing (the contrast of these images has been adjusted for display purposes only), and (b) scatter plot showing FD and 7-AAD intensities per volume in a representative set of analyzed images.

2.6. Confirming and Calibration of the Fluorescence Imaging Method

The fluorescence-imaging method was compared to flow-cytometry data from previous work on two-pulse DC EP (53). For the same conditions (E_1= 1 kV/cm, t_1= 1 ms and E_2= 0.1 - 0.8 kV/cm, t_2= 30 ms), the fluorescence-imaging results were consistent with the prior data.

A calibration experiment was performed in order to correlate the fluorescence intensity measured in EP-mediated molecular delivery experiments with the concentration of the delivered molecules. We designed an array of rectangular micro-chambers with 20 μm height using double-sided adhesive tape (Nitto Denko America Inc, Teaneck, NJ) as a spacer between two cover slips (VWR). Serial dilutions of FD in electroporation buffer ranging between 0.312 - 50.0 μM where imaged at room temperature to generate calibration curves of FD intensity versus concentration for both 10 kDa and 70 kDa FD conjugates. All the measurements have been performed 3-4 times for each case in order to obtain consistent results.

Figure 2.4 shows the fluorescence intensity per volume for both 10 kDa and 70 kDa FD concentration. A linear correlation was observed for both 10 kDa and 70 kDa FD in the concentration range analyzed in this study. The cell Fluorescence intensity per volume was then converted to the concentration using the calibration curves. Such calibration experiments have been performed by other investigators, see e.g. [38].

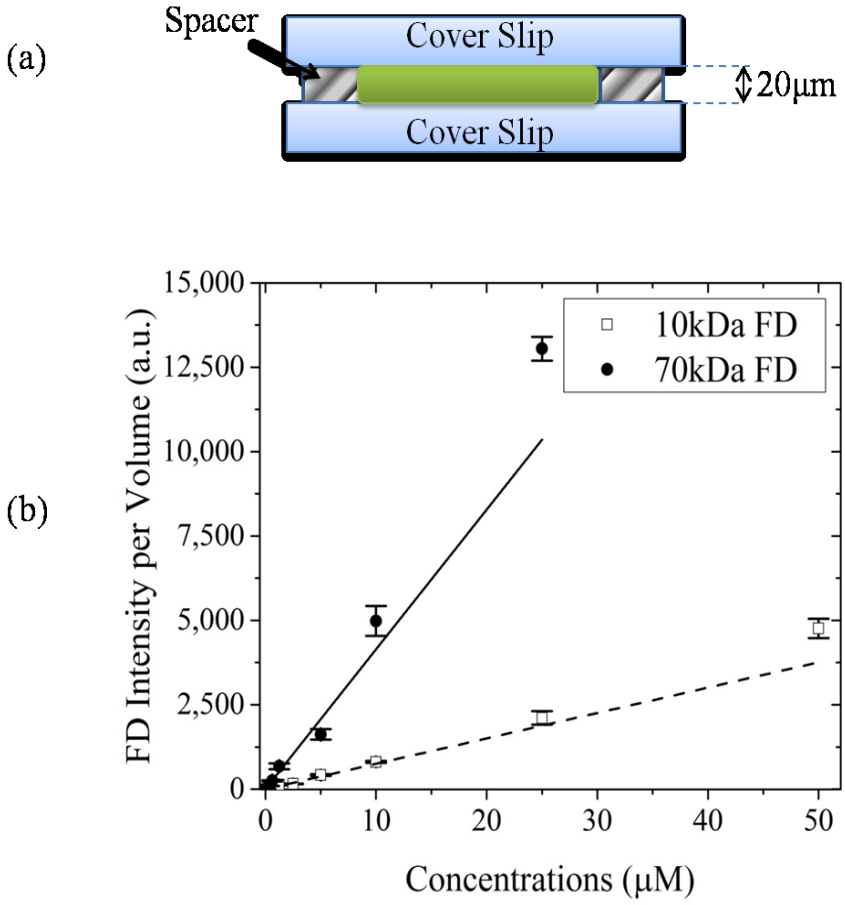

Figure 2.4. Calibration experiment, (a) the schematic of placing different-diluted FD solutions. The gap between cover slips is fixed by using double-sided adhesive tape. (b) The fluorescence intensity versus concentration for FD 10k and FD 70k conjugates.

Chapter 3

Results

In this chapter of the thesis, experimental results are presented. Although, the main scope of this study is on the two-pulse EP method, two different set of single-pulse experiments are conducted in order to determine pulsing parameters. Later, two-pulse EP experimental results are presented in two main categories depending on the delay time between the two pulses: (I) no delay, and (II) various delay times ranging from 1 ms to 300 s.

3.1. Single AC Pulse Application

In the two-pulse EP procedure, although the FP is considered in many studies to only permeabilize the cell membrane, a considerable amount of molecular delivery can occur due to electrophoretic effects of the DC FP that is typically used [15,17,19,20,22,27]. As seen in Figure 3.1, after a single DC pulse (E_1=0.90 kV/cm, t_1=1 ms), a significant amount of 10 kDa FD is delivered into the cell. On the other hand, an AC pulse greatly reduces 10 kDa FD delivery. The lack of delivery at the end of the AC pulse is due to non-binding nature of FD molecules, since electrophoretically-driven FD molecules may enter into the cells during the pulsation, but also leave the cell due to alternating polarity of AC field. Increasing the frequency of the AC field further reduces 10 kDa FD delivery. Here, the 10 kHz AC FP was judged to have negligible (<10%) delivery compared to that of the two-pulse case with no delay. Therefore, to clearly separate permeabilization from delivery, we employed a 10 kHz AC FP with E_1=0.90 kV/cm and t_1=1 ms.

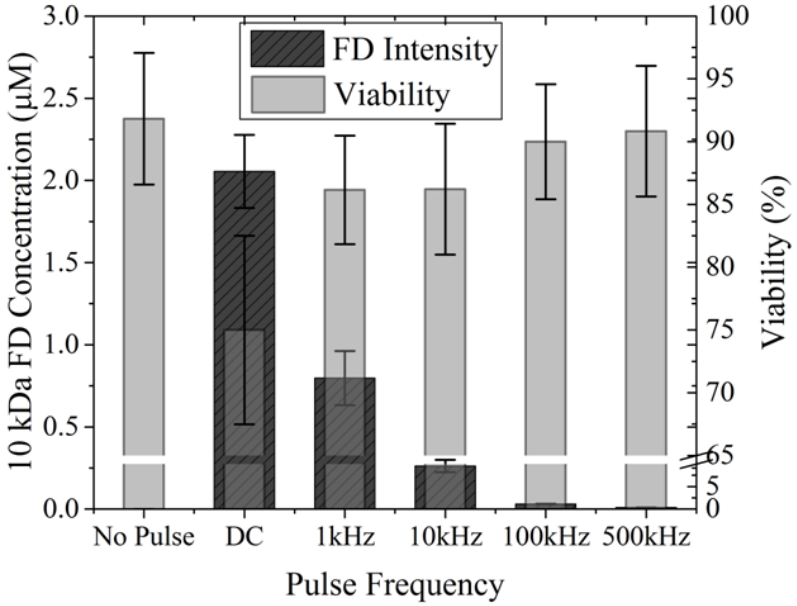

Figure 3.1. Intracellular 10 kDa concentrations and viability for different-frequency AC fields (1 ms, 0.9 kV/cm) compared to a DC field of the same strength.

3.2. Single DC Pulse Application

In order to determine the field strength of the SP, we first applied 30-ms-long single DC pulses with different field strengths. As seen in Figure 3.2 there is a slight 10 kDa FD uptake (around 0.25 μM) beginning at 0.40 kV/cm. This is presumably the threshold DC field strength which would begin to permeabilize the 3T3 cells for 10 kDa FD in our experiments. Since the objectives of this work were to study the effect of FP-to-SP delay time on membrane resealing and molecular delivery, we wanted the SP not to create new pores, but only to hold the electropores open and provide the electrophoretic force for delivery. Therefore the SP's field strength was chosen to be 0.33 kV/cm, lower than threshold required for significant electroporation and delivery by a single DC pulse and both SP field strength and duration are kept fixed (E_2=0.33 kV/cm, t_2= 30 ms) for all

cases. In this way, we can isolate the effect of the FP and correlate the amount of delivery obtained after the SP with the permeabilization level of the membrane achieved by the FP.

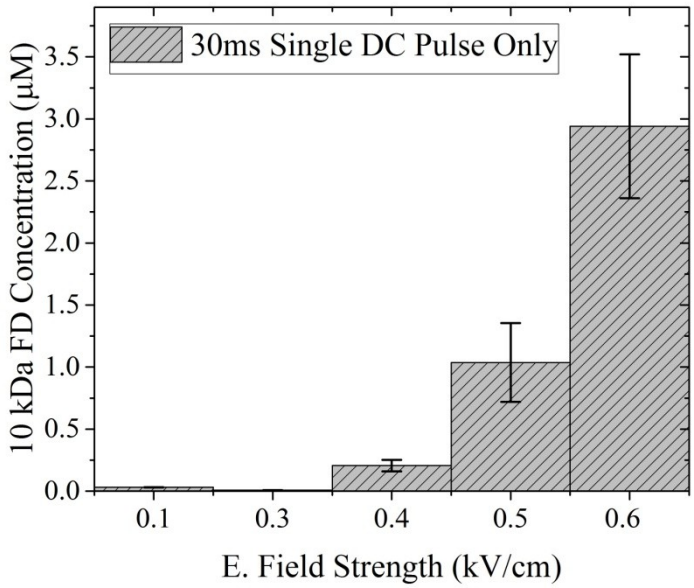

Figure 3.2. Delivered intracellular concentration for a single 30-ms-long DC pulse of different field strengths.

3.3. Two-Pulse Application with No Delay

We first consider a two-pulse protocol consisting of an AC FP (10 kHz, E_1=0.9 kV/cm, t_1=1 ms) immediately followed by a DC SP. The weak DC SP by itself is not of sufficient strength to cause adequate EP for 10 kDa FD. Figure 3.3 shows the delivered intra-cellular FD concentration for the FP-only and two-pulse cases. It can be seen that applying the FP only does not cause any significant FD delivery, and the intra-cellular concentration remains almost the same in spite of increasing FP field strength or changing molecule size. However, applying the DC SP (E_2= 0.33 kV/cm, t_2= 30 ms) with no-delay achieves a relatively high molecular delivery ranging from 1 μM to 4 μM for the 10 kDa FD (Figure 3.3). Hence a clear separation of permeabilization and delivery is

obtained by using an AC FP followed by a DC SP. Moreover, the two-pulse protocol delivers FD with viabilities exceeding 70% in the 10 kDa case.

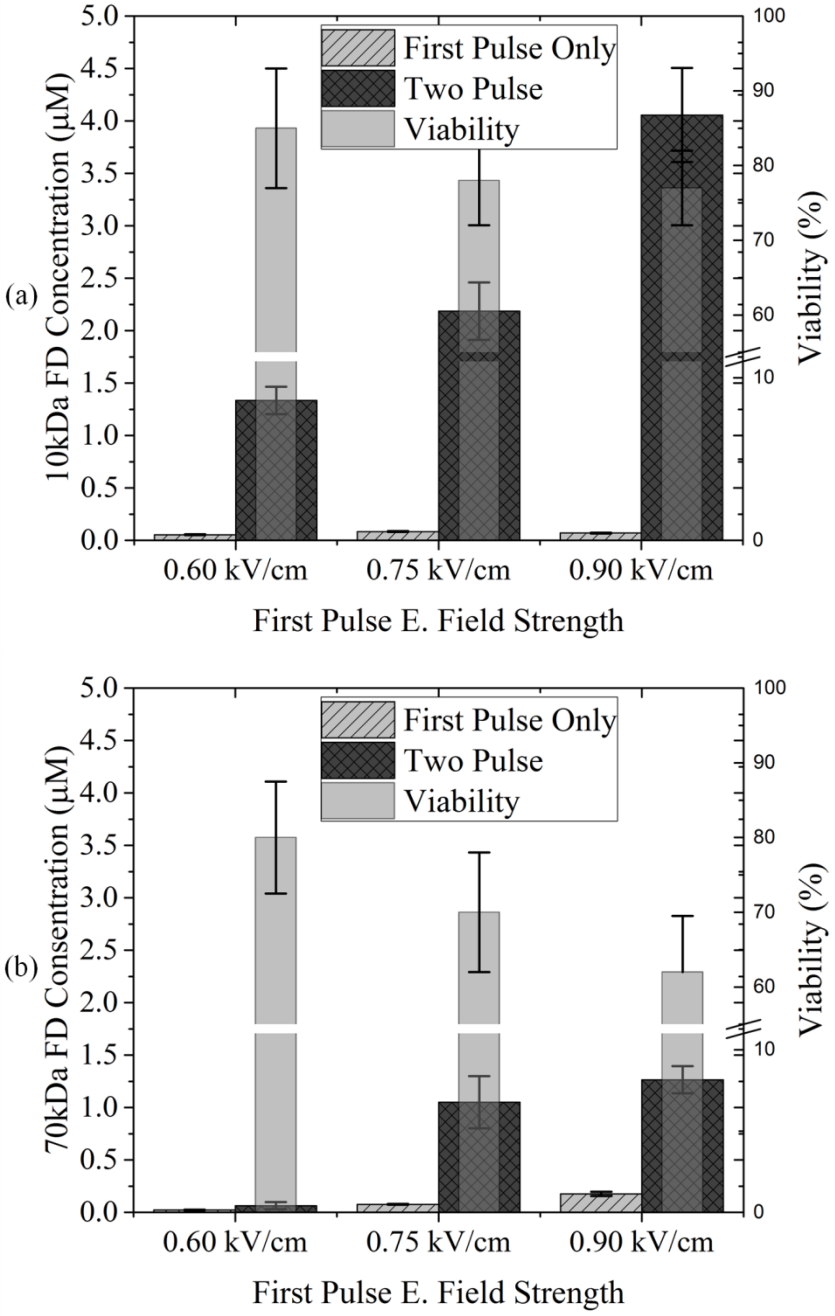

Figure 3.3. Delivered intra-cellular FD concentrations and viability for different AC FP strengths and molecule sizes: (a) 10 kDa FD and (b) 70 kDa FD.

Having achieved a clear separation of permeabilization and delivery, we next examine the degree of permeabilization by applying FPs of different field strengths (E_1= 0.6 - 0.9 kV/cm, t_1= 1 ms). As seen in Figure 3.3 the different columns of, different FP strengths between 0.6 kV/cm to 0.9 kV/cm result in very different FD-delivery levels when followed by the same SP. As expected, increasing the field strength of the FP increases intra-cellular FD concentration, presumably due to increased permeabilization of the cell membrane. This result shows the importance of the FP in the two-pulse EP protocol, since the final delivery amounts strongly depends on the FP field strength, even though the FP itself achieves negligible delivery.

We next investigated the effect of molecular size on the delivery achieved by two-pulse EP. Comparing Figure 3.3a with Figure 3.3b, we see that delivered intra-cellular concentrations of two different-sized FD molecule (10 kDa and 70 kDa) are very different under the same conditions. For example, with a 0.6 kV/cm FP immediately followed by a SP (E_2=0.33 kV/cm, t_2= 30 ms), there is considerable delivery of 10 kDa FD (around 1.25 μM). However, with the same pulsing parameters, there is negligible intra-cellular delivery of 70 kDa FD. This suggests that pores formed by the 0.6 kV/cm FP have a pore-size distribution that allows 10 kDa FD molecules to pass through, but very few 70 kDa FD molecules. We interpret this to mean that the size distribution of electroporated pores shifts to larger pores with higher FP field strength. Finally, with a 0.9 kV/cm-field-strength FP, the delivery of 10 kDa FD is almost doubled over that of the 0.75 kV/cm case, while the 70 kDa delivery increases slightly. This difference shows that increase in the formation of larger electropores is less than of smaller electropores in the

jump in FP strength from 0.75 to 0.9 kV/cm. The data clearly indicate that pulsing parameters (in particular the FP strength) need to be adjusted for target-molecule size.

Summarizing briefly, our results without delay between the pulses indicate that the FP is instrumental in creating adequate permeabilization to facilitate the transport of the molecules via the SP, although the FP by itself effects negligible delivery by design.

3.4. Two-Pulse Application with Variable Delay

In reversible EP, electropores eventually disappear and the cell membrane reseals to return to its preshock state post-pulsation. In other words, the cell membrane becomes impermeable for foreign molecules long enough post-pulsation. This resealing stage of reversible EP typically takes longer than permeabilization, e.g. electropermeabilization can occur in micro or nano-seconds with suitable pulsation, while the disappearance of the electropores has been reported to take seconds or minutes [81,82]. If long resealing times hold, post-pulsation delivery can be of significance for transfection efficiency, particularly for small molecules of high diffusivity. We took advantage of the separation between permeabilization and delivery offered by our AC+DC two-pulse protocol design to study transport dynamics by delaying the SP by times ranging from 1 ms to 300 s. The total delivery of the two sizes of FD could be measured to infer the permeability of the membrane to the target molecules after various delay times of the SP. Figure 3.4 shows the measured intra-cellular FD concentrations shown versus the delay times between pulses for 10 kDa and 70 kDa FD. It can be seen that there is a nearly 50% drop in the FD concentration with 100 ms delay between first and second pulses due to resealing for most of the cases. However, (reduced) delivery persists even when the SP is delayed by up to hundreds of seconds. (Recall that the SP by itself is too weak to permeabilize and

deliver.) Furthermore, comparing the data in Figure 3.4a, for different intensity FPs, we see that the rate of delivery decrease with delay times actually depends on the field strength of the FP. For the 0.6 kV/cm FP, negligible 10 kDa FD delivery is obtained after around 100 s of delay between the pulses, but for the 0.75 and 0.9 kV/cm FPs, complete cessation of delivery by the SP only occurs after delays of thousands seconds. Additionally, the slopes of fitted line are also different for different permeabilization degrees (particularly for 10 kDa cases). The change in delivered intracellular concentration (and by inference the resealing rate) is higher in the highly permeabilized cases. This suggests that the resealing dynamics are directly related with the permeabilization degree, and that although a complete resealing takes minutes, a significant portion of resealing happens in very short time post-pulsation.

In Figure 3.4, it can be clearly seen that the delivery of both 10 kDa and 70 kDa FD decreases nearly linearly with the logarithm of the delay time regardless of the molecule size. Although, comparing Figure 3.4a and b, for instance, at 0.75 kV/cm FP case, very little 70 kDa FD is delivered after SP delays of 100 s or 300 s, the smaller 10 kDa molecule continues to be delivered after similar delay times. This suggests that even at the same permeabilization level, the exclusion times where the electropores are impermeable for the target molecule may vary depending on the molecule size. According to our experimental conditions, in general, this exclusion time for the 70 kDa FD is around 100-300 s, and for the smaller 10 kDa FD the exclusion time is predicted to be more than thousand seconds depending on the FP strength. It can be also interpreted as that the electropores allowing entry of 10 kDa FD (but not 70 kDa FD) persist for time gaps on the order of 100 s between the FP and SP. In addition to that, the intra-cellular

concentration decrease-rates (inferred to resealing-rates) vary strongly with FP strength for 10 kDa FD but not for 70 kDa FD, as seen in Figure 3.4b. The 10 kDa case (Figure 3.4a) shows that the variation of intracellular concentration with the delay time has different slopes depending on the strength of the FP. However, for the 70 kDa FD case, the 0.75 and 0.9 kV/cm FP lines have almost the same slope. This shows that the EP-mediated molecular transport for the different-sized target molecules has different dynamic depending on the current permeabilization state.

Briefly, our results with various delay times between the pulses indicate that, the resealing time of the membrane strongly depends on the permeabilization degree, and a significant drop in the delivery occurs within very short time due to resealing process. Additionally, the transport dynamic of different-sized molecules varies, however the decrease of the intra-cellular concentration with respect to delay times has a linear logarithmic behavior regardless of the target molecule size.

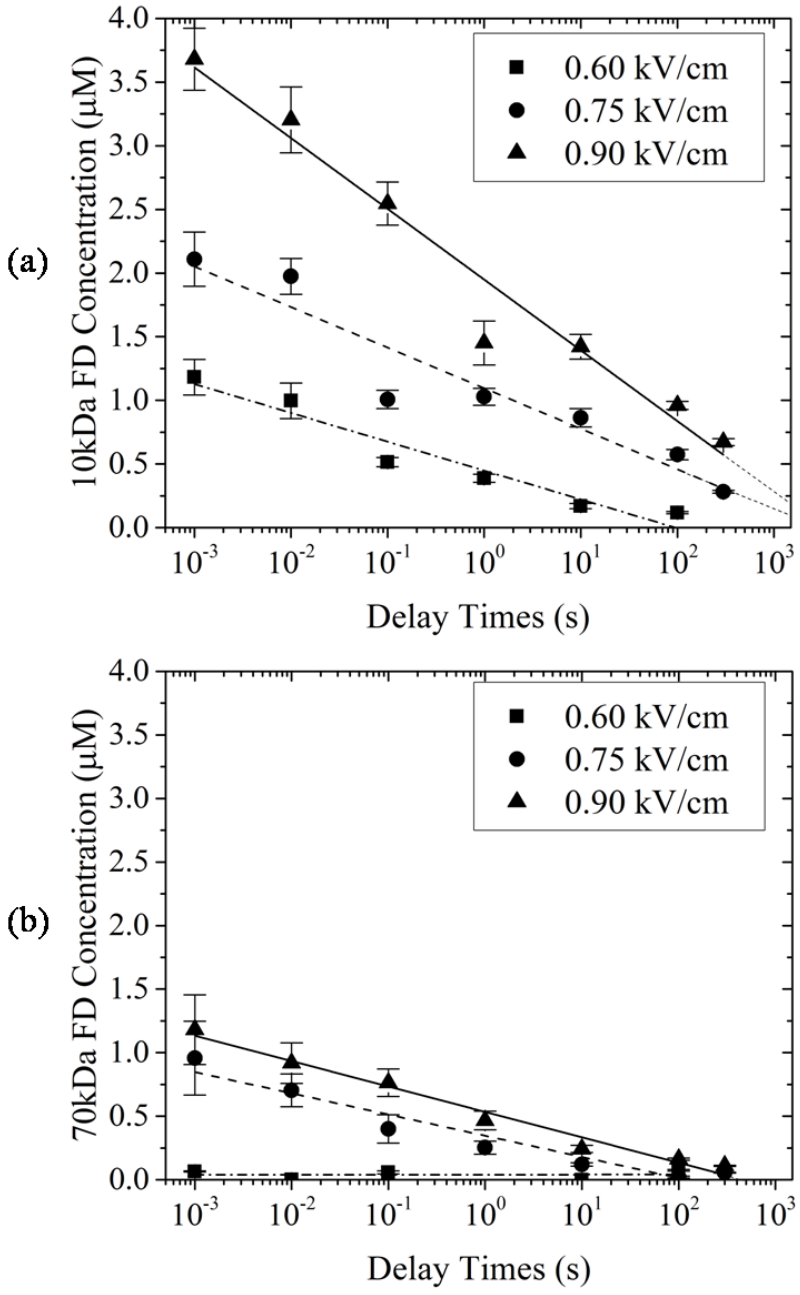

Figure 3.4. Delivered intra-cellular FD concentrations with different delay times ranging from 1 ms to 300 s for different AC FP strengths and molecule sizes: (a) 10 kDa FD and (b) 70 kDa FD.

Chapter 4

Discussion

Experimentally, two techniques have been commonly used to determine the degree of cell-membrane permeabilization by electric pulses: (I) measuring the conductance or current change across the cell [28,47,83–86], and (II) measuring the transport of marked molecules. For quantifying the size of pores, the second method is more attractive because different-sized molecules can be used [38]. However, this method is somewhat restricted in that it must deliver a sufficient amount of target molecule in order to acquire signal, *i.e.*, it is actually sensitive to delivery and not permeabilization [43,45,87]. Therefore, membrane permeabilization is traditionally considered in tandem with molecular delivery, although the two phenomena are distinct and involve different physical mechanisms. In this work, we performed two-pulse EP using an 10 kHz AC-field FP, which was shown to permeabilize the membrane with minimal net electrophoretic delivery of FD and a 0.33 kV/cm filed strength of DC SP, which was also shown not to permeabilize the membrane itself but to provide electrophoretic force for the delivery. By this means, we were able to probe the degree of permeabilization according to delivery amount after the SP.

It is shown that in two-pulse EP protocol, the FP affects the delivery amount obtained after the SP crucially. Our results, which showed that increasing the AC FP field strength increases the degree of permeabilization, are in agreement with previous studies [18,20,23,26,28]. In those studies, EP efficiency increased with the FP strength until a critical point where the efficiency started to decrease due to low viability. Knowing that

fact, in our study, further high field strengths have not been applied for the FP, since the viability ratios were aimed to maintain above 60% throughout the experiments. Distinctively, we have used two different-sized FD molecules (10 kDa and 70 kDa) which were provided us to infer the distribution of electropore size and number for different degree of permeabilization. By using different-sized molecules, Saulis et al. was performed a study in order to investigate the size of electropores that created by different pulsing parameters [45]. However those target molecules were small molecules (MW< 4 kDa), thus, besides electrophoresis, the dynamic diffusive effect was also involved in transport mechanism. Therefore we have used a mid-sized FD molecules weighted 10 kDa and 70 kDa in order to avoid diffusive process and to have a similar size range with RNA or peptides and more accurate quantification of delivery which directly correlated with the permeabilization level were obtained [19,38]. Additionally, by taking advantage of non-binding nature of the FD molecules, a clear separation of permeabilization and delivery was achieved and the complexities in transport mechanism such as DNA-membrane interactions were avoided.

In this work, it is seen that the transport of large molecules (70 kDa) requires stronger FP field strength in order to obtain a significant delivery. One of the few studies that focused on the formation and distribution of electropores as a model study by Krassowska and Filev et al. explained the theoretical background of this behavior [72]. In their model, increasing the field strength extended the pore size and increased the number of pores, but the formation rate of large pores was slower than the formation of the small pores. Therefore, when comparing a highly and a moderately permeabilized cells, it is possible that the number of large pores would be nearly equal, while the number of small

pores would be much higher in the highly permeabilized cell. Our results are consistent with the predicted evolution of size distribution of the electropores with field strength, showing delivery of 70 kDa FD at a FP strength of 0.75 kV/cm, while no delivery was observed for 0.60 kV/cm. That shows the size of electropores is extended with increasing the field strength. Furthermore, when the FP strength is further increased from 0.75 kV/cm to 0.90 kV/cm, the delivery increment for 10 kDa FD was higher than for the 70 kDa molecule. In light of these findings, we can speculate that delivery of large molecules, such as transport of gene or big-sized drugs or proteins, requires stronger pulse strength while a slightly above the critical permeabilization threshold pulse strength may have a better efficiency than a higher electric field strength, since almost the same amount of delivery will be achieved with higher viability ratio. However, the optimum electric-field strength is likely to be cell and molecule dependent.

Another important stage for reversible electroporation is the resealing or disappearance of the electropores [11,14,81,88]. Incomplete resealing is an indicator of cell mortality since dead cells cannot recover from their leaky state. Numerous researchers have measured membrane resealing times using various methods, with results ranging from milliseconds to minutes. Membrane-resealing times inferred from measuring the membrane conductance [36,47,86,89] tend to be shorter (short-term resealing) than the times suggested by uptake of small [13,44,45,90–92] or larger molecules [93,94] after pulsation (long-term resealing). For instance, Hibino et al. showed one of the first sub-second methods using voltage-sensitive membrane dye [36], and later on H. He et al. and Khine et al. developed two sub-second methods to measure resealing times. All concluded that membrane resealing occurred on timescales on the

order of milliseconds [47,86]. In other studies, a test molecule was added to the cell solution at different time post-pulsation, and the exclusion times of the target molecule was correlated with resealing. This method provides an actual resealing time, but, due to the difficulty in precisely controlling the addition of the test molecule for very short times, measurement of the resealing dynamics at the sub-second level is impossible. Our current work takes advantage of a two-pulse protocol with an AC permeabilization FP followed by a DC delivery pulse to probe membrane resealing over a wide range of timescales. A similar delayed SP method was used by Sukharev et al. earlier to probe the interaction of DNA with electropores [15]. It was observed that the transfection efficiency decreased with increasing of the delay time which is consistent with our results. However, distinct from that work, our studies utilize an AC FP, and varied the strength of FP [15]. This variation of the FP strength, in other words, variation of the degree of permeabilization, yielded us information that resealing rates depend on the FP. As shown in Figure 3.4a, with 0.9 kV/cm FP case resealing-rate is faster than the others. As stated above, highly permeabilized cells have higher number of small pores, and as expectedly small pores reseals faster while the large pores may cause some defects on the membrane. Thus, we can hypothesize that, electropores shrink rather quickly, but nano-sized pores or defects tend to remain for a much longer time. This also agrees with Krassowska and Filev et al. [72] in their model, all pores shrunk to minimum-energy level pore size (around 0.8 nm) immediately after pulsation while they persisted until a complete resealing. These nano-sized pores or defects act as nucleation sites when the SP pulse is applied. Therefore, taking advantage of low energy barrier of nucleation sites for poration, the SP extends the pore sizes, although the SP itself is not enough for permeabilization. However, with the

same FP and SP, but with different delay times the delivery amounts vary strongly. That means, although the SP extends the nano-sized pores, it cannot reporate the resealed pores. Therefore, the decrease in the delivery with increasing delay time can be correlated with resealing dynamics of the electropores. The different exclusion times for 10 kDa and 70 kDa FD indicates the pore shrinking time, since between 100-300 s delay time pores shrink to exclude 70 kDa and then more than thousands seconds to exclude 10 kDa FD molecules depending on the FP strength.

In the previous studies, Andre et al. [18] indicated that a delay time between pulses is necessary. They stated that with a HV FP cell membrane reaches a highly permeabilized state and then with a no-delay SP cell membrane overporates, and consequently lowers the viability and transfection efficiency. They claim that a delay time between pulses allow the cell membrane to recover from a highly permeabilized state, but electro-transfection can continue due to slow resealing process. Therefore, taking advantage of the slow resealing process, a SP provides an electrophoretic force for delivery and increase the efficiency. Firstly, in that work, DNA electro-transfection was studied which involves DNA-membrane interaction mechanism besides electrophoresis, thus the effect of the delay time is not clear. Although for high field strength FP, a delay time between pulses might be helpful for the viability, but the total pore area shrinks significantly in short time period post-pulsation. Thus the advantageous of the high permeabilization degree is forfeited. Additionally, it is also shown in our work that for delivering large-sized-molecules (like DNA, RNA, proteins, etc.), increasing the strength of the FP slightly increased the delivery efficiency, therefore a high strength FP is not necessary. In another work by Satkauskas et al. [16] the effect of delay time between

pulses is investigated ranging from 5 ms to 10,000 s and showed that an optimal efficiency reached between 0.3 - 100 s delay times. They claim that, even though a high permeabilization degree is achieved after the FP, the DNA solution needs more time for a better redistribution within the tissue. However, longer delay times (more than 300 s) decreases the transfection of DNA. Additionally, they emphasize the importance of a SP in order to increase transfection efficiency. Our results also agree with that work, since a great portion of delivery achieved after the SP and a long delay time decreased the transfection drastically. Contrary, we observed almost 50%-drop of the delivery within 100 ms delay. The reason behind this conflict might be due to the complexity of the DNA electro-transfection which involves DNA-membrane interaction or redistribution of the DNA solution within the tissue (as indicated in that work). In our study, by using non-binding FD, we have avoided these complexities and directly correlated the decrease of delivery with resealing process.

As previously seen in Figure 3.4, the total delivered intracellular concentration depends on the logarithm of the delay time regardless of the molecule size. In the many literature, the delivery amounts decreased with long enough delay times [15,16,79], however, according to our knowledge, a logarithmic behavior have not been observed. We speculate this to mean that around 50% of resealing happened in the first 100 ms while complete resealing took hundreds of seconds. Although the physical mechanisms behind this behavior are not understood yet, these results suggesting resealing is both a short-term and long-term process may explain the enormous differences in the literature for membrane resealing times.

Chapter 5

Conclusion

In this work, we have conducted a series of two-pulse electroporation experiments, focusing on delivery efficiency of two different-sized molecules using different pulsing parameters. Distinct work, we have employed an AC field FP to achieve a clear separation of permeabilization and delivery, and we have also varied the delay times between the AC FP and DC SP systematically. When the SP was kept at a fixed strength (chosen to be below the critical permeabilization threshold) and the FP field strength was varied, the delivery of 10 kDa and 70 kDa varied strongly. At lower field strengths of 0.6 kV/cm, membrane pores generated by the AC FP were sufficiently large to allow transport of 10 kDa FD, but not 70 kDa FD. Increasing AC FP field strength increases the size and number of electropores on the membrane, allowing delivery of the larger molecule. We further systematically studied the effect of delay times between pulses on the delivery efficiency. Using the AC FP to porate the membrane, and a DC SP for transport, we are able to probe resealing dynamics over timescales ranging from milliseconds to minutes. We find for these cells and pulsing parameters that the EP-mediated delivery scales with the logarithm of the delay time regardless of the molecule size and 50% of resealing happens in the first 100 ms after pulsation, however complete resealing takes hundreds of seconds. This result may harmonize the inconsistent membrane resealing times reported in the literature for different experiments.

First of all this study demonstrated that molecular delivery of two-pulse EP decreases logarithmically with the delay time between pulses regardless of molecular size,

where the physical foundation behind have not understood yet. Therefore a more detailed study on this finding can be considered as a future work by delivering more different-sized target molecule and using different types of cells. In addition to that, this logarithmic behavior can be validated with another fluorescence analyzing method such as flow-cytometry. Furthermore, a clear evidence for the fast shrinking after the pulsation could not presented with our current experiment design. A new experimental procedure can be designed to probe the transport mechanism in shorter time scales.

Appendix A

Image analysis code

Image analysis code presented below:

```
clc
clear all
close all

cumResults2=zeros(0,1);
cumResults3=zeros(0,1);
diameters=zeros(0,1);
filter_values=zeros(0,1);
stds=zeros(0,1);

genel_result=zeros(0,3);

% Change the folder name
img_dir = strcat('E:\Experiment results\Yasir\Cuvette\New
folder_58\02kV\Bright');
    dirOutput = dir ([img_dir '\capture*.tif']);
fileNames = {dirOutput.name}';
numFrames = numel (fileNames);

img_dir2 = strcat('E:\Experiment results\Yasir\Cuvette\New folder_58\02kV\FD');
    dirOutput = dir ([img_dir2 '\capture*.tif']);
fileNames2 = {dirOutput.name}';

img_dir3 = strcat('E:\Experiment results\Yasir\Cuvette\New
folder_58\02kV\7AAD');
    dirOutput = dir ([img_dir3 '\capture*.tif']);
fileNames3 = {dirOutput.name}';

for i=3:numFrames
    close all
% Takes the pictures in memory
I = imread([img_dir,'/',fileNames{i}]);
I2 = imread([img_dir2,'/',fileNames2{i}]);
I3 = imread([img_dir3,'/',fileNames3{i}]);

% Adjusts the contrast of pictures
J = imadjust (I);
% J2 = imadjust (I2);
J3 = imadjust (I3);

% figure('units','normalized','outerposition',[0 0 1 1])

subplot(2,2,3), subimage(I3, [525 1200])
subplot(2,2,2), subimage(I2, [525 2125])
subplot(2,2,1), subimage(J)
% subplot(2,2,3), subimage(J)

% Pops up the picture which is taken in bright field

% Starts calculating the density of each cell
while(1)
while(1)
```

```
[xc,yc]=ginput(1);        % Click on the center of each cell
   % Rounds the center coordinates
   Rxc=round(xc);
   Ryc=round(yc);
   % Converts the picture into double form
   AA=double(J);
   AAA=mat2gray(AA);

   % Creates the lines for Left, Right, Down and Up limits
   Xleft=[AAA(Ryc, 1:Rxc)];
   Xright=[AAA(Ryc, Rxc:end)];
   Ydown=[AAA(Ryc:end, Rxc)];
   Yup=[AAA(1:Ryc, Rxc)];

   % Determines the size of Left wing
   for j=1:size(Xleft,2)
       if 20+j>= size(Xleft,2)
           XL=20;
       elseif Xleft((Rxc-20)-j)>=0.75
           XL=j+25;
           break
       end
   end
   % Determines the size of Right wing
   for j=1:size(Xright,2)
       if 20+j>= size(Xright,2)
           XR=20;
       elseif Xright(20+j)>=0.75
           XR=j+25;
           break
       end
   end
   % Determines the size of Up wing
   for j=1:size(Yup,1)
       if 20+j>= size(Yup,1)
           YU=20;
       elseif Yup((Ryc-20)-j)>=0.75
           YU=j+25;
           break
       end
   end
   % Determines the size of Down wing
   for j=1:size(Ydown,1)
       if 20+j>= size(Ydown,1)
           YD=20;
       elseif Ydown(20+j)>=0.75
           YD=j+25;
           break
       end
   end

   % Determines new corrected cell center
   xDiameter= (XL+XR);
   x_diff= (xDiameter/2)-XL;
   new_xc= round(Rxc+ x_diff);
   yDiameter= (YD+YU);
   y_diff= (yDiameter/2)-YU;
   new_yc= round(Ryc+ y_diff);

  % Calculates the diameter
   if xDiameter>=xDiameter
       diameter=xDiameter;
   else
```

```
        diameter=yDiameter;
    end
    hold on
    % Plots the cell center
    plot(new_xc, new_yc, 'r+');

    % Draws the circle around the cell

    DrawCircle(new_xc, new_yc, diameter/2, 32, 'y-');

    % Asks you if the circle is drawed well
    choice = questdlg('Do you think it is fine', ...
    'Good Circles', ...
    'No Repeat','Yes it is','Yes it is');
    % Handle response
    switch choice
        case 'No Repeat'
        m = 1;
        case 'Yes it is'
        m = 2; % Continues the intensity computation
    end
    if m==2
    break
    end
end
    % Starts computing the intensity
   % Gather the all results
   radius= round(diameter/2);

   diameters=[diameters;diameter];
%    filter_values=[filter_values; filteration];
%    stds=[stds; std];

   results_unfitered=meanDisk(I2, new_xc, new_yc, radius);
   results2=results_unfitered;
   cumResults2=[cumResults2;results2];


   results_unfitered3=meanDisk(I3, new_xc, new_yc, radius);
   results3=results_unfitered3;
   cumResults3=[cumResults3;results3];
%

   % Asks you to proceed to other picture
    choice = questdlg('Do you want to proceed the next picture', ...
    'Next Picture', ...
    'Not Yet','Yes I am Done','Not Yet');
    % Handle response
    switch choice
        case 'Not Yet'
        m = 1;
        case 'Yes I am Done'
        m = 2; % Proceeds the next picture
    end
    if m==2
    break
    end

end
end
genel_result=[diameters, cumResults2, cumResults3];
```

Function that used for drawing circle is given below.

```
function DrawCircle(x, y, r, nseg, S)
% Draw a circle on the current figure using ploylines
%  INPUT: (x, y, r, nseg, S)
%  x, y:    Center of the circle
%  r:       Radius of the circle
%  nseg:    Number of segments for the circle
%  S:       Colors, plot symbols and line types


theta = 0 : (2 * pi / nseg) : (2 * pi);
pline_x = r * cos(theta) + x;
pline_y = r * sin(theta) + y;

plot(pline_x, pline_y, S);
```

Function that used for computing the mean intensity of a disk shape is given below.

```
function [m sd mask] = meanDisk(img, xc, yc, r)
%meanDisk computes mean of values inside a circle
%   M = meanDisk(IMG, XC, YC, R) returns the mean of IMG(Y,X) for all X and
%   Y such that the Euclidean distance of (X,Y) from (XC,YC) is less than
%   R. IMG must be 2-D, R must be positive, and some elements of IMG must
%   lie within the circle.
% This section is for efficiency only - avoids wasting computation time on
% pixels outside the bounding square
[sy sx] = size(img);
xmin = max(1, floor(xc-r));
xmax = min(sx, ceil(xc+r));
ymin = max(1, floor(yc-r));
ymax = min(sy, ceil(yc+r));
img = img(ymin:ymax, xmin:xmax); % trim boundaries
xc = xc - xmin + 1;
yc = yc - ymin + 1;
% Make a circle mask
[x y] = meshgrid(1:size(img,2), 1:size(img,1));
mask = (x-xc).^2 + (y-yc).^2 < r.^2;
% Compute mean
m = sum(sum(double(img) .* mask)) / sum(mask(:));
sd = sqrt(sum(sum((double(img).*mask-m*mask).^2))/sum(mask(:)));
%sd = sqrt(sum((double(img).*mask-m*mask).^2)/sum(mask(:)));
end
```

References

[1] E. Neumann, M. Schaefer-Ridder, Y. Wang, P.H. Hofschneider, Gene transfer into mouse lyoma cells by electroporation in high electric fields., EMBO J. 1 (1982) 841–845.

[2] J. Teissie, N. Eynard, M.C. Vernhes, A. Benichou, V. Ganeva, B. Galutzov, et al., Recent biotechnological developments of electropulsation. A prospective review, Bioelectrochemistry. 55 (2002) 107–112.

[3] R. Heller, S. Shirley, S. Guo, A. Donate, L. Heller, Electroporation based gene therapy—From the bench to the bedside, in: Eng. Med. Biol. Soc. EMBC 2011 Annu. Int. Conf. IEEE, IEEE, 2011: pp. 736–738.

[4] J. Teissie, J.M. Escoffre, A. Paganin, S. Chabot, E. Bellard, L. Wasungu, et al., Drug delivery by electropulsation: Recent developments in oncology, Int. J. Pharm. 423 (2012) 3–6.

[5] M. Golzio, M.P. Rols, J. Teissie, In vitro and in vivo electric field-mediated permeabilization, gene transfer, and expression, Methods. 33 (2004) 126–135.

[6] L.M. Mir, M.F. Bureau, J. Gehl, R. Rangara, D. Rouy, J.-M. Caillaud, et al., High-efficiency gene transfer into skeletal muscle mediated by electric pulses, Proc. Natl. Acad. Sci. 96 (1999) 4262–4267.

[7] M. Costa, M. Dottori, K. Sourris, P. Jamshidi, T. Hatzistavrou, R. Davis, et al., A method for genetic modification of human embryonic stem cells using electroporation, Nat. Protoc. 2 (2007) 792–796.

[8] D. Miklavčič, D. Šemrov, H. Mekid, L.M. Mir, A validated model of in vivo electric field distribution in tissues for electrochemotherapy and for DNA electrotransfer for gene therapy, Biochim. Biophys. Acta BBA-Gen. Subj. 1523 (2000) 73–83.

[9] L.M. Mir, P.H. Moller, F. André, J. Gehl, Electric Pulse-Mediated Gene Delivery to Various Animal Tissues, Adv. Genet. 54 (2005) 83–114.

[10] E. Neumann, A.E. Sowers, C.A. Jordan, Electroporation and electrofusion in cell biology, Springer, 1989.

[11] J. Gehl, Electroporation: theory and methods, perspectives for drug delivery, gene therapy and research, Acta Physiol. Scand. 177 (2003) 437–447.

[12] J.C. Weaver, Electroporation theory, in: Anim. Cell Electroporation Electrofusion Protoc., Springer, 1995: pp. 3–28.

[13] E. Neumann, S. Kakorin, K. Toensing, Principles of membrane electroporation and transport of macromolecules, in: Electrochemother. Electrogenether. Transdermal Drug Deliv., Springer, 2000: pp. 1–35.

[14] F. Andre, L.M. Mir, DNA electrotransfer: its principles and an updated review of its therapeutic applications, Gene Ther. 11 (2004) S33–S42.

[15] S.I. Sukharev, V.A. Klenchin, S.M. Serov, L.V. Chernomordik, C. YuA, Electroporation and electrophoretic DNA transfer into cells. The effect of DNA interaction with electropores, Biophys. J. 63 (1992) 1320–1327.

[16] S. Satkauskas, M.F. Bureau, M. Puc, A. Mahfoudi, D. Scherman, D. Miklavcic, et al., Mechanisms of in vivo DNA electrotransfer: respective contributions of cell electropermeabilization and DNA electrophoresis, Mol. Ther. 5 (2002) 133–140.

[17] M. Pavlin, K. Flisar, M. Kandušer, The role of electrophoresis in gene electrotransfer, J. Membr. Biol. 236 (2010) 75–79.
[18] F.M. André, J. Gehl, G. Sersa, V. Préat, P. Hojman, J. Eriksen, et al., Efficiency of high-and low-voltage pulse combinations for gene electrotransfer in muscle, liver, tumor, and skin, Hum. Gene Ther. 19 (2008) 1261–1272.
[19] M.M. Sadik, M. Yu, M. Zheng, J.D. Zahn, J.W. Shan, D.I. Shreiber, et al., Scaling Relationship and Optimization of Double-Pulse Electroporation, Biophys. J. 106 (2014) 801–812.
[20] M.F. Bureau, J. Gehl, V. Deleuze, L.M. Mir, D. Scherman, Importance of association between permeabilization and electrophoretic forces for intramuscular DNA electrotransfer, Biochim. Biophys. Acta. 1474 (2000) 353–359.
[21] S. Satkauskas, F. André, M.F. Bureau, D. Scherman, D. Miklavcic, L.M. Mir, Electrophoretic component of electric pulses determines the efficacy of in vivo DNA electrotransfer, Hum. Gene Ther. 16 (2005) 1194–1201.
[22] M. Kandušer, D. Miklavčič, M. Pavlin, Mechanisms involved in gene electrotransfer using high-and low-voltage pulses—an in vitro study, Bioelectrochemistry. 74 (2009) 265–271.
[23] L.C. Heller, M.J. Jaroszeski, D. Coppola, A.N. McCray, J. Hickey, R. Heller, Optimization of cutaneous electrically mediated plasmid DNA delivery using novel electrode, Gene Ther. 14 (2007) 275–280.
[24] S. Haberl, M. Kandušer, K. Flisar, D. Hodžić, V.B. Bregar, D. Miklavčič, et al., Effect of different parameters used for in vitro gene electrotransfer on gene expression efficiency, cell viability and visualization of plasmid DNA at the membrane level, J. Gene Med. 15 (2013) 169–181.
[25] N. Pavselj, V. Préat, DNA electrotransfer into the skin using a combination of one high- and one low-voltage pulse, J. Control. Release Off. J. Control. Release Soc. 106 (2005) 407–415.
[26] J. Yockell-Lelièvre, V. Riendeau, S.N. Gagnon, C. Garenc, M. Audette, Efficient transfection of endothelial cells by a double-pulse electroporation method, DNA Cell Biol. 28 (2009) 561–566.
[27] T. Stroh, U. Erben, A.A. Kühl, M. Zeitz, B. Siegmund, Combined pulse electroporation–a novel strategy for highly efficient transfection of human and mouse cells, PloS One. 5 (2010) e9488.
[28] D. Cukjati, D. Batiuskaite, F. André, D. Miklavčič, L.M. Mir, Real time electroporation control for accurate and safe in vivo non-viral gene therapy, Bioelectrochemistry. 70 (2007) 501–507.
[29] C. Faurie, M. Rebersek, M. Golzio, M. Kanduser, J.-M. Escoffre, M. Pavlin, et al., Electro-mediated gene transfer and expression are controlled by the life-time of DNA/membrane complex formation, J. Gene Med. 12 (2010) 117–125.
[30] R. Stämpfli, Reversible electrical breakdown of the excitable membrane of a Ranvier node, Acad Bras Cienc. 30 (1958) 57–63.
[31] K. Kinosita Jr., T.Y. Tsong, Voltage-induced conductance in human erythrocyte membranes, Biochim. Biophys. Acta BBA - Biomembr. 554 (1979) 479–497.
[32] T.S. Santra, P.-C. Wang, F.G. Tseng, Electroporation Based Drug Delivery and Its Applications, (2013).

[33] K. Kinosita Jr, I. Ashikawa, N. Saita, H. Yoshimura, H. Itoh, K. Nagayama, et al., Electroporation of cell membrane visualized under a pulsed-laser fluorescence microscope, Biophys. J. 53 (1988) 1015–1019.
[34] R.L. Vincelette, C.C. Roth, M.P. McConnell, J.A. Payne, H.T. Beier, B.L. Ibey, Thresholds for phosphatidylserine externalization in chinese hamster ovarian cells following exposure to nanosecond pulsed electrical fields (nsPEF), PloS One. 8 (2013) e63122.
[35] B. Flickinger, T. Berghöfer, P. Hohenberger, C. Eing, W. Frey, Transmembrane potential measurements on plant cells using the voltage-sensitive dye ANNINE-6, Protoplasma. 247 (2010) 3–12.
[36] M. Hibino, H. Itoh, K. Kinosita Jr, Time courses of cell electroporation as revealed by submicrosecond imaging of transmembrane potential, Biophys. J. 64 (1993) 1789–1800.
[37] M. Hibino, M. Shigemori, H. Itoh, K. Nagayama, K. Kinosita Jr, Membrane conductance of an electroporated cell analyzed by submicrosecond imaging of transmembrane potential, Biophys. J. 59 (1991) 209–220.
[38] D.A. Zaharoff, J.W. Henshaw, B. Mossop, F. Yuan, Mechanistic analysis of electroporation-induced cellular uptake of macromolecules, Exp. Biol. Med. 233 (2008) 94–105.
[39] G. Pucihar, T. Kotnik, D. Miklavčič, J. Teissié, Kinetics of transmembrane transport of small molecules into electropermeabilized cells, Biophys. J. 95 (2008) 2837–2848.
[40] P.J. Canatella, J.F. Karr, J.A. Petros, M.R. Prausnitz, Quantitative study of electroporation-mediated molecular uptake and cell viability, Biophys. J. 80 (2001) 755–764.
[41] B. Gabriel, J. Teissie, Direct observation in the millisecond time range of fluorescent molecule asymmetrical interaction with the electropermeabilized cell membrane, Biophys. J. 73 (1997) 2630–2637.
[42] H. He, D.C. Chang, Y.-K. Lee, Using a micro electroporation chip to determine the optimal physical parameters in the uptake of biomolecules in HeLa cells, Bioelectrochemistry. 70 (2007) 363–368.
[43] M.R. Prausnitz, B.S. Lau, C.D. Milano, S. Conner, R. Langer, J.C. Weaver, A quantitative study of electroporation showing a plateau in net molecular transport, Biophys. J. 65 (1993) 414–422.
[44] M.-P. Rols, J. Teissié, Electropermeabilization of mammalian cells to macromolecules: control by pulse duration, Biophys. J. 75 (1998) 1415–1423.
[45] G. Saulis, R. Saulė, Size of the pores created by an electric pulse: Microsecond vs millisecond pulses, Biochim. Biophys. Acta BBA-Biomembr. 1818 (2012) 3032–3039.
[46] J. Teissie, M.-P. Rols, An experimental evaluation of the critical potential difference inducing cell membrane electropermeabilization, Biophys. J. 65 (1993) 409–413.
[47] H. He, D.C. Chang, Y.-K. Lee, Nonlinear current response of micro electroporation and resealing dynamics for human cancer cells, Bioelectrochemistry. 72 (2008) 161–168.

[48] J.A. Lundqvist, F. Sahlin, M.A. \AAberg, A. Strömberg, P.S. Eriksson, O. Orwar, Altering the biochemical state of individual cultured cells and organelles with ultramicroelectrodes, Proc. Natl. Acad. Sci. 95 (1998) 10356–10360.
[49] M.R. Prausnitz, C.D. Milano, J.A. Gimm, R. Langer, J.C. Weaver, Quantitative study of molecular transport due to electroporation: uptake of bovine serum albumin by erythrocyte ghosts, Biophys. J. 66 (1994) 1522–1530.
[50] T. Kotnik, G. Pucihar, M. Reberšek, D. Miklavčič, L.M. Mir, Role of pulse shape in cell membrane electropermeabilization, Biochim. Biophys. Acta BBA-Biomembr. 1614 (2003) 193–200.
[51] G. Pucihar, L.M. Mir, D. Miklavčič, The effect of pulse repetition frequency on the uptake into electropermeabilized cells in vitro with possible applications in electrochemotherapy, Bioelectrochemistry. 57 (2002) 167–172.
[52] E. Neumann, Membrane electroporation and direct gene transfer, Bioelectrochem. Bioenerg. 28 (1992) 247–267.
[53] C. Faurie, E. Phez, M. Golzio, C. Vossen, J.-C. Lesbordes, C. Delteil, et al., Effect of electric field vectoriality on electrically mediated gene delivery in mammalian cells, Biochim. Biophys. Acta BBA-Biomembr. 1665 (2004) 92–100.
[54] D. Miklavcic, L. Towhidi, Numerical study of the electroporation pulse shape effect on molecular uptake of biological cells, Radiol. Oncol. 44 (2010) 34–41.
[55] G. Pucihar, T. Kotnik, M. Kandušer, D. Miklavčič, The influence of medium conductivity on electropermeabilization and survival of cells in vitro, Bioelectrochemistry. 54 (2001) 107–115.
[56] G.L. Prasanna, T. Panda, Electroporation: basic principles, practical considerations and applications in molecular biology, Bioprocess Eng. 16 (1997) 261–264.
[57] P. Hojman, H. Gissel, F.M. Andre, C. Cournil-Henrionnet, J. Eriksen, J. Gehl, et al., Physiological effects of high-and low-voltage pulse combinations for gene electrotransfer in muscle, Hum. Gene Ther. 19 (2008) 1249–1260.
[58] M.M. Sadik, J. Li, J.W. Shan, D.I. Shreiber, H. Lin, Quantification of propidium iodide delivery using millisecond electric pulses: Experiments, Biochim. Biophys. Acta BBA-Biomembr. 1828 (2013) 1322–1328.
[59] K.H. Schoenbach, S.J. Beebe, E.S. Buescher, Intracellular effect of ultrashort electrical pulses, Bioelectromagnetics. 22 (2001) 440–448.
[60] J. Teissie, N. Eynard, B. Gabriel, M.P. Rols, Electropermeabilization of cell membranes, Adv. Drug Deliv. Rev. 35 (1999) 3–19.
[61] J.A. Nickoloff, Animal cell electroporation and electrofusion protocols, Springer, 1995.
[62] T. Tryfona, M.T. Bustard, Enhancement of biomolecule transport by electroporation: a review of theory and practical application to transformation of Corynebacterium glutamicum, Biotechnol. Bioeng. 93 (2006) 413–423.
[63] R.E. Neal, R.V. Davalos, The feasibility of irreversible electroporation for the treatment of breast cancer and other heterogeneous systems, Ann. Biomed. Eng. 37 (2009) 2615–2625.
[64] R. Nuccitelli, U. Pliquett, X. Chen, W. Ford, R.J. Swanson, S.J. Beebe, et al., Nanosecond pulsed electric fields cause melanomas to self-destruct, Biochem. Biophys. Res. Commun. 343 (2006) 351–360.

[65] B. Rubinsky, G. Onik, P. Mikus, Irreversible electroporation: a new ablation modality--clinical implications, Technol. Cancer Res. Treat. 6 (2007) 37–48.
[66] K.H. Schoenbach, R.P. Joshi, R.H. Stark, F.C. Dobbs, S.J. Beebe, Bacterial decontamination of liquids with pulsed electric fields, IEEE Trans. Dielectr. Electr. Insul. 7 (2000) 637–645.
[67] T. Kotnik, P. Kramar, G. Pucihar, D. Miklavcic, M. Tarek, Cell membrane electroporation- Part 1: The phenomenon, IEEE Electr. Insul. Mag. 28 (2012) 14–23.
[68] S.M. Becker, A.V. Kuznetsov, Local temperature rises influence in vivo electroporation pore development: a numerical stratum corneum lipid phase transition model, J. Biomech. Eng. 129 (2007) 712–721.
[69] J. Teissie, M. Golzio, M.P. Rols, Mechanisms of cell membrane electropermeabilization: a minireview of our present (lack of?) knowledge, Biochim. Biophys. Acta BBA-Gen. Subj. 1724 (2005) 270–280.
[70] T.R. Gowrishankar, D.A. Stewart, J.C. Weaver, Model of a confined spherical cell in uniform and heterogeneous applied electric fields, Bioelectrochemistry. 68 (2006) 181–190.
[71] R.P. Joshi, Q. Hu, K.H. Schoenbach, Dynamical modeling of cellular response to short-duration, high-intensity electric fields, IEEE Trans. Dielectr. Electr. Insul. 10 (2003) 778–787.
[72] W. Krassowska, P.D. Filev, Modeling electroporation in a single cell, Biophys. J. 92 (2007) 404–417.
[73] M. Joergensen, B. Agerholm-Larsen, P.E. Nielsen, J. Gehl, Efficiency of Cellular Delivery of Antisense Peptide Nucleic Acid by Electroporation Depends on Charge and Electroporation Geometry, Oligonucleotides. 21 (2011) 29–37.
[74] J. Li, W. Tan, M. Yu, H. Lin, The effect of extracellular conductivity on electroporation-mediated molecular delivery, Biochim. Biophys. Acta BBA-Biomembr. 1828 (2013) 461–470.
[75] M.S. Venslauskas, S. Šatkauskas, R. Rodaitė-Riševičienė, Efficiency of the delivery of small charged molecules into cells in vitro, Bioelectrochemistry. 79 (2010) 130–135.
[76] J. Teissié, J. Escoffre, M. Rols, M. Golzio, Time dependence of electric field effects on cell membranes. A review for a critical selection of pulse duration for therapeutical applications, Radiol. Oncol. 42 (2008) 196–206.
[77] M. Golzio, J. Teissié, M.-P. Rols, Direct Visualization at the Single-Cell Level of Electrically Mediated Gene Delivery, Proc. Natl. Acad. Sci. U. S. A. 99 (2002) 1292–1297.
[78] V.A. Klenchin, S.I. Sukharev, S.M. Serov, L.V. Chernomordik, Chizmadzhev YuA, Electrically induced DNA uptake by cells is a fast process involving DNA electrophoresis, Biophys. J. 60 (1991) 804–811.
[79] H. Wolf, M.P. Rols, E. Boldt, E. Neumann, J. Teissié, Control by pulse parameters of electric field-mediated gene transfer in mammalian cells, Biophys. J. 66 (1994) 524–531.
[80] J.B. Little, Quantitative Studies of Radiation Transformation with the A31-11 Mouse BALB/3T3 Cell Line, Cancer Res. 39 (1979) 1474–1480.
[81] G. Saulis, Pore disappearance in a cell after electroporation: theoretical simulation and comparison with experiments, Biophys. J. 73 (1997) 1299–1309.

[82] K.A. DeBruin, W. Krassowska, Modeling electroporation in a single cell. I. Effects of field strength and rest potential, Biophys. J. 77 (1999) 1213–1224.
[83] U. Pliquett, H. Krassen, C.G. Frantescu, D. Wesner, E. Neumann, K. Schoenbach, Asymmetric changes in membrane conductance due to hyper-and depolarization: probing with current and voltage clamp, in: IFMBE Proc, 2005: p. 1923.
[84] H. Krassen, U. Pliquett, E. Neumann, Nonlinear current–voltage relationship of the plasma membrane of single CHO cells, Bioelectrochemistry. 70 (2007) 71–77.
[85] L.V. Chernomordik, S.I. Sukharev, S.V. Popov, V.F. Pastushenko, A.V. Sokirko, I.G. Abidor, et al., The electrical breakdown of cell and lipid membranes: the similarity of phenomenologies, Biochim. Biophys. Acta BBA-Biomembr. 902 (1987) 360–373.
[86] M. Khine, C. Ionescu-Zanetti, A. Blatz, L.-P. Wang, L.P. Lee, Single-cell electroporation arrays with real-time monitoring and feedback control, Lab. Chip. 7 (2007) 457–462.
[87] S.M. Kennedy, Z. Ji, J.C. Hedstrom, J.H. Booske, S.C. Hagness, Quantification of electroporative uptake kinetics and electric field heterogeneity effects in cells, Biophys. J. 94 (2008) 5018–5027.
[88] J.C. Weaver, Y.A. Chizmadzhev, Theory of electroporation: a review, Bioelectrochem. Bioenerg. 41 (1996) 135–160.
[89] Y. Zhou, J. Shi, J. Cui, C.X. Deng, Effects of extracellular calcium on cell membrane resealing in sonoporation, J. Control. Release Off. J. Control. Release Soc. 126 (2008) 34–43.
[90] E. Tekle, R.D. Astumian, P.B. Chock, Electroporation by using bipolar oscillating electric field: an improved method for DNA transfection of NIH 3T3 cells., Proc. Natl. Acad. Sci. 88 (1991) 4230–4234.
[91] M. Kandušer, M. Šentjurc, D. Miklavčič, Cell membrane fluidity related to electroporation and resealing, Eur. Biophys. J. 35 (2006) 196–204.
[92] B. Gabriel, J. Teissié, Control by electrical parameters of short- and long-term cell death resulting from electropermeabilization of Chinese hamster ovary cells, Biochim. Biophys. Acta BBA - Mol. Cell Res. 1266 (1995) 171–178.
[93] T.D. Xie, L. Sun, T.Y. Tsong, Study of mechanisms of electric field-induced DNA transfection. I. DNA entry by surface binding and diffusion through membrane pores, Biophys. J. 58 (1990) 13–19.
[94] S. Yumura, R. Matsuzaki, T. Kitanishi-Yumura, Introduction of macromolecules into living Dictyostelium cells by electroporation, Cell Struct. Funct. 20 (1995) 185–190.